IL NUOVO CIMENTO Vol. 26 C, N. 1 Gennaio-Febbraio 2003

Solar cycles reflected in the English climate

E. C. Njau

Physics Department, University of Dar es Salaam - P.O. Box 35063, Dar es Salaam, Tanzania

(ricevuto il 22 Ottobre 2001; revisionato il 9 Maggio 2002; approvato l' 1 Luglio 2002)

Summary. — We show that patterns of variations in the central England temperature since 1660 as well as rainfall in England and Wales since 1726 contain dominant oscillations and switching sequences at the periods of some sunspot cycles. These particular sunspot cycles are: the 80–90 year sunspot cycle, the 22-year sunspot cycle, and the 11-year sunspot cycle. In particular, the variation patterns are switched from one form into another form at a switching period of 80–90 years. Solar cycles of relatively larger periodicities are also dominantly reflected in southeast Scotland temperature records since 1125 A.D. and in California temperature records since 3431 B.C. We also show that some large and rapid changes in central England and California temperature variations are associated with solar activity.

PACS 92.60.Ry – Climatology.
PACS 96.60.Vg – Particle radiation, solar wind.
PACS 96.40.Kk – Solar modulation and geophysical effects.

1. – Introduction

The third and latest assessment report of the Intergovernmental Panel on Climate Change (IPCC) was released in 2001 (see ref. [1]). This report concludes in part that natural factors have made small contributions to radiative forcing over the past century. This conclusion implies that the combined change in radiative forcing of the two major natural factors (*i.e.* solar variations and volcanic aerosols) has been small over the past century. According to the IPCC report mentioned above, the reason why the IPCC did write-off solar activity as a major player in the cause of climate changes is lack of "mechanisms for amplification of solar effects on climate that have rigorous theoretical and observational basis". In this paper we report that influences of solar effects have dominated on the temperature and rainfall variation patterns in England since 1700, as well as on temperature variations in California since 3431 B.C.

2. – Analysis

Instrument rainfall records in England are available dating as far back as some years after 1676 when Richard Towneley produced the first raingauge in England. Besides

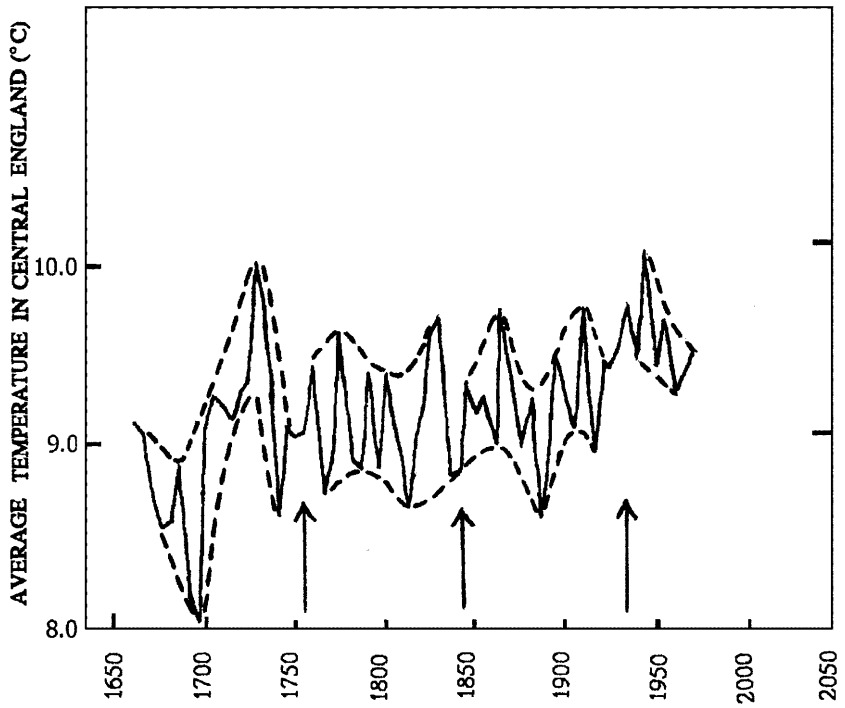

Fig. 1. – A plot of average temperature in central England from 1660 up to 1970 (solid lines) as reported in Lamb [2]. Discontinuous lines have been used to sketch the amplitude-modulation envelopes of the temperature variations using standard curve-fitting methods [5]. A change from one form of amplitude-modulation envelope to a different envelope is indicated by an arrow-headed line.

instrument temperature records in central England are available dating as far back as about 1860. This availability of instrument temperature data follows applications of the invention of the thermometer in Italy by Galilei Galileo in the first half of the seventeenth century.

Lamb [2] reports a wealth of central England temperature records which stretch back to 1660. These records were taken in over 43 stations in central England, noting that this region has the longest continuous record of daily weather in the world. Besides, Manley [3] reports a wealth of rainfall in England and Wales which stretch back to 1726. Rainfall data has been recorded in most of the English, Welsh and Scottish counties, involving 217 meteorological and climatological stations. For the period before availability of the respective scientific instruments, the rainfall and temperature records mentioned above and also the other records used in this paper were reconstructed from proxy data, weather registers and dairies, farm and estate records, and chronicles. It should be stressed that the temperature and rainfall records used in this paper are not all instrument records. However, all those rainfall and temperature records used in this paper which were collected before instrumental periods have already been rendered comparable with those to be obtained by modern standard techniques of exposure as explained in Lamb [4]. Let us start our analysis with temperature records for central England.

Average temperature variations in the central England stations mentioned earlier

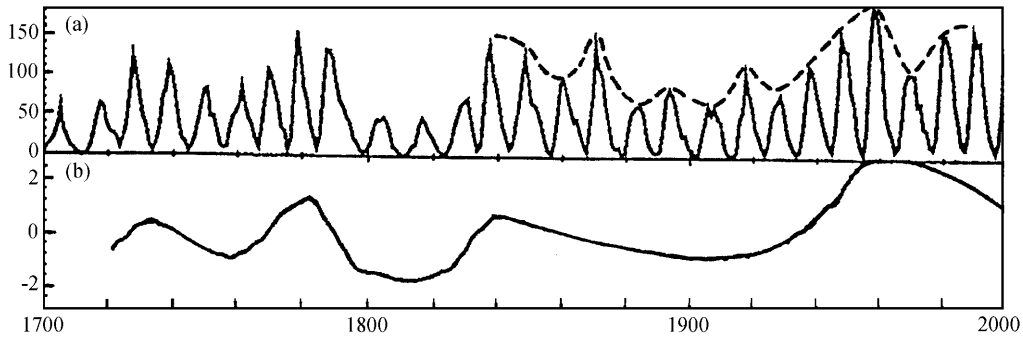

Fig. 2. – A plot of: a) yearly sunspot numbers series from 1700 to 2000 as reported in ref. [6], and b) instantaneous peak-to-peak amplitude of the variations in a) after filtering out variations with periods smaller than 40 years. Note also that the latter variations which are filtered out from b) have been approximately sketched in a) from 1840 using a discontinuous line.

in this section from 1660 up to 1970 have been graphically plotted in Lamb [2]. We took these graphical representations of temperature variations and sketched out their amplitude-modulation envelopes as follows. Firstly we used the latest curve-fitting techniques [5] to fit discontinuous-line curves along the maximum points of the temperature variations. Secondly we used the latest curve-fitting techniques [5] to fit discontinuous-line curves along the minimum points of the temperature variations. The results of this exercise are shown in fig. 1.

What we clearly see in fig. 1 is a series of different and approximately sinusoidal amplitude-modulation envelopes. Each sinusoidal envelope is different from the others either in amplitude or in modulating frequency. The space separating any two adjoining envelopes is shown by an arrow-headed line. This space contains intermediate changes through which an amplitude-modulation envelope changes into a different envelope. Let us compare the sinusoidal amplitude-modulation envelopes in fig. 1 with the sunspot-number oscillations in fig. 2, noting that backward extensions of the two plots in figs. 2(a) and (b) would in each case reach the first (zero-level) minimum at the year 1690. Variations in solar activity are measured by many indices (*e.g.*, magnetic activity, prominences, faculae, solar flares, corona, etc.), but most of these are reasonably correlated with the relative sunspot number (*i.e.* number of dark spots on the Sun's disc) introduced by Wolf in 1847. It is on the basis of this correlation and the availability of long records of sunspot number that the latter is used as a measure of solar activity. Variations in sunspot number take the form of some nearly cyclic or quasi-cyclic changes normally referred to as "sunspot cycles" or "solar cycles". As reported in detail in refs. [7, 8], analysis of the available long records of sunspot numbers has shown that solar cycles exist at the following periods: $5\frac{1}{2}$ years, $\sim$ 11-years, 22-years, 35–40 years, 80–90 years, 170–200 years, $\sim$ 400 years, $\sim$ 1700 years and $\sim$ 2000 years. Since changes that result in the variation or modulation of the sunspot number also induce (at least very small) variations in the solar constant, the sunspot cycle periodicities listed above are expected to feature at least very slightly in the solar constant pattern.

There are apparently two causes of the 22-years solar cycle (or double sunspot cycle or Hale cycle as it is alternatively called). Firstly this cycle appears in the amplitude-modulating pattern of the 11-years solar cycle (*e.g.*, see the discontinuous line in fig. 2(a) from 1860 to 1930). This amplitude-modulating pattern expectedly gives rise to tiny

TABLE I. – *Matching minima and maxima in the temperature envelopes in fig.* 1 *and the sunspot number oscillation in fig.* 2(b).

Parameter	Years of minima	Years of maxima
Temperature envelope	1690, ****, 1810	1730, 1780
Sunspot-number oscillation	1690, 1758, 1810	1730, 1780

**** Discontinuation of the first envelope in 1740 apparently prevented this envelope from normally reaching its next minimum.

variations in the "solar constant" at the period of the double sunspot cycle. Secondly the physical significance of the double sunspot cycle is in the fact that the Sun's magnetic field reverses its polarity with each new (11-years) sunspot cycle. Thus any resulting Sun-Weather relationships may possibly be through the solar wind.

As clarified further by table I, the sunspot number oscillation in fig. 2(b) varies in unison with the sinusoidal amplitude-modulation envelopes in fig. 1 from 1690 up to 1840.

We worked out the correlation coefficient between the curve in fig. 2(b) up to 1840 and the mean of the corresponding lower and upper discontinuous lines in fig. 1. The value of correlation coefficient (at 99.9% statistical significance level) arrived at is +0.74.

After the year 1840, the apparent temperature-sunspot relationship changes into a different form. For example, the envelope stretching from 1840 to 1925 in fig. 1 oscillates at frequency $(2/3)f_0$, where f_0 is the corresponding frequency of the discontinuous line in fig. 2(a). Between 1860 and 1930, this discontinuous line has a consistent period of 22 years. To verify the temperature-sunspot relationship shown above, note that while the latter discontinuous line oscillates through $1\frac{1}{2}$ cycles between 1870 and 1907, the corresponding temperature envelope in fig. 1 goes through only one complete cycle over the same period. Justification for the temperature-sunspot relationship just mentioned may be obtained from previous works. As an example, for any variation in sunspot numbers at frequency F, large oscillations at frequency $(2/3)F$ are expectedly set up in terrestrial temperature through some "amplifying" mechanism in the surface-atmosphere system [7]. Following the envelope stretching from 1840 to 1925, there is a transition period stretching from 1925 to 1958. What follows this transition period is another envelope which starts with a maximum in 1958 and then appears to proceed with frequency $(2/3)f_0$, where f_0 is the frequency of the discontinuous line in fig. 2(a). What is even more interesting is that the period at which the temperature envelopes in fig. 1 change or switch into different forms (*i.e.* the time distance between adjacent arrow-headed lines) is in the 85–90 years range. This range overlaps well with the period of the 80–90 years sunspot cycle.

It would seem that an amplitude-modulation envelope in fig. 1 changes or switches into a different envelope when the sunspot variations associated with it change into sufficiently different frequency (or frequencies). To illustrate and justify this point, let us start at the extreme leftward arrowed line in fig. 1 and move towards the right-hand side. Firstly we note that the oscillation in fig. 2(b) has a different period before the timing of the extreme left-hand side arrowed line in fig. 1 compared with the period after this line. Between the latter arrowed line and the year 1840, the oscillation in fig. 2(b) has a period of about 58 years. But after 1840 the latter oscillation changes into a relatively much larger period. It so happens that after a 1940–1950 intermediate time-

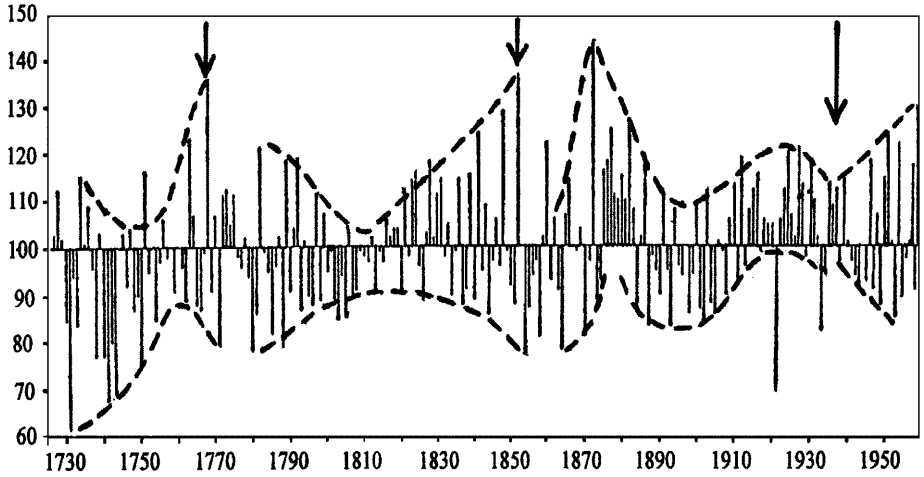

Fig. 3. – General rainfall in England and Wales (thin, solid vertical lines) as a percentage of the 1881–1915 average from 1726 to 1960 as reported in Manley [3]. Discontinuous lines have been used to sketch out the amplitude-modulation envelopes of the rainfall variations using standard curve-fitting methods [5]. The timings of large-scale changes in the amplitude-modulation envelope are shown by arrowed lines.

zone, the 1760-to-1840 envelope changes into the different 1850-to-1924 envelope in fig. 1. As far as the latter envelope is concerned, the associated sunspot number variation (*i.e.* discontinuous line in fig. 2(a)) has a period of 22 years. From 1938 onwards, the latter discontinuous line acquires a period much larger than 22 years. As expected, what then follows is that after a 1924–1938 transitional zone, the 1850-to-1924 envelope switches into a different envelope (see fig. 1). So the picture obviously gathered here is that an amplitude-modulation envelope in fig. 1 changes into a different envelope whenever the associated oscillation in fig. 2 changes its period(s). Therefore the arrowed lines in figs. 1 and 3 apparently show timings at which associated solar variations (see fig. 2) undergo sufficiently large frequency changes.

The solar influences on England temperature described above are somehow almost similarly mapped onto England rainfall (fig. 3). This figure displays rainfall variations averaged over the England and Welsh stations mentioned earlier in this paper. The latter figure shows that the rainfall variations in England and Wales from 1726 to 1960 are in a series of sinusoidal and node-antinode forms of amplitude-modulation envelopes which change into each other at a period of about 86 years, which is in the range of the period of the 80–90 years sunspot cycle. Each minimum (or node) in fig. 3 coincides with a minimum in fig. 1. In particular, the amplitude-modulation envelope in fig. 1 which stretches from 1860 to 1920 varies approximately in phase with the corresponding envelope in fig. 3. Also from 1730 up to 1850, the amplitude-modulation envelopes in fig. 3 vary in unison with the sunspot number oscillation in fig. 2(b). Note that the two minima in the latter oscillation at about the years 1760 and 1810 coincide with nodes in fig. 3.

Simple forward extrapolation of fig. 3 using the information given above shows that the rainfall patterns in this figure would currently be at or close to a large anti-node. This probably explains why the autumn and winter of 2000/01 were wettest on record

over England and Wales, with widespread and unprecedented flooding [9].

The last amplitude-modulation envelope in fig. 1 started in 1944. This particular envelope slopes down after the latter year apparently to some minimum located sometime after 1970, and which is not shown in fig. 1 due to unavailability of the relevant data. Since the starting phase and envelope-thickness of this particular envelope appear to be follow-up continuations of the ending phase and envelope-thickness, respectively, of the previous envelope, it would seem that the transition from the latter envelope to the next envelope merely introduced an increase in the constant component level probably with some phase change. Indeed this is evident from visual inspections of fig. 1. Consequently it would be expected that the last and last but one envelopes in fig. 1 are characterised by similar sunspot-temperature relationships.

On the basis of the account given above and also since the last envelope in fig. 1 reaches the next minimum in the mid-1980s (*e.g.*, data comparable to Lamb's data and available in the Tiempo Climate website www.cru.uea.ac.uk/tiempo/newswatch/as on 12/06/2001), we would normally expect the ongoing warming in England to stop and reverse during the early years of this century. There is need, though, to find out conclusively if the much-publicised global warming due to human activities can or cannot overshadow and hence nullify this expected natural temperature reversal. Unfortunately this exercise cannot be done using computer climate models which are incapable of properly simulating the mechanisms for the apparent amplification of solar effects on climate change (*e.g.*, see ref. [7]). According to ref. [7], human activities can cause climate changes equal to those caused by solar effects only if they can give rise to radiative effects equivalent to those caused by about 20% of the constant component of earthward solar energy, the so-called "solar constant".

The Sun-Weather relationships for England already presented in this paper supplement previous results on England already given by other workers using different approaches and leading to different conclusions. Among these other results are those given by Hargreaves [10] in which the central England July temperature and lightning or thunderstorms in England correlated positively with the 22-year sunspot cycle and the 11-year sunspot cycle, respectively. It was noted in a subsequent report [8] that 11-year oscillations are dominantly present in the records of annual rainfall and temperature at Oxford between 1815 and 1962.

Just for comparison purposes, it is worth noting that records from other parts of the northern hemisphere display dominant Sun-Weather relationships [8, 13]. This is shown in the representative illustrations given in figs. 4 and 5. From 1900 onwards, the major sinusoidal oscillations in fig. 4 (see thick solid line) and fig. 5 (see the smooth curve) have a common period that is equal to that of the second harmonic of the solar oscillation in fig. 2(b). Note that the rather rapid rise in temperature shown in fig. 5 from about 1970 onwards coincides with the rising phase of the sinusoidal oscillation in this figure. The same observation has been noted with regard to global mean temperature with the exception that the sinusoidal oscillation involved has a period equal to that of the solar cycle in fig. 2(b) (see ref. [8]). Simple forward extrapolation on fig. 5 implies then that the next major minimum in this figure will expectedly coincide with the next minimum in fig. 2(b). This implies that some cooling trend is expected in the northern hemisphere during the early years of this century as already noted in connection with England temperature.

Some physical mechanisms that can adequately explain the Sun-Weather relationships presented in the text of this paper have been detailed in ref. [7]. A simplified summary of these mechanisms is given in the Appendix.

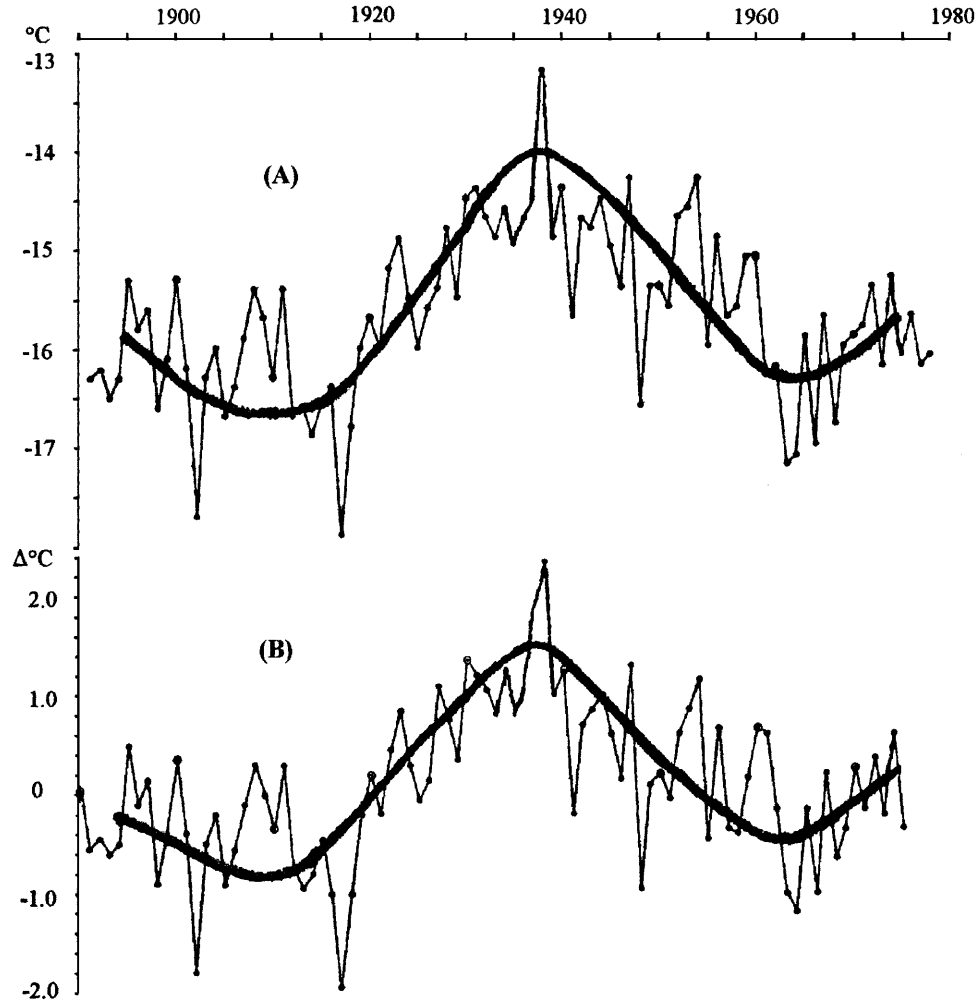

Fig. 4. – A plot in thin solid lines of: a) mean annual surface air temperature for the zone 77.50 °N to 82.5 °N from 1890 through to 1978; and b) departures (in C) of mean annual surface air temperature for the zone 72.5 °N to 87.5 °N from a long-term mean. The averages of the temperature variations in a) and b) have been plotted using thick solid lines. Data for the thin solid line plots in both a) and b) above have been adapted from Kukla and Robinson [11].

Clearly the dominant sinusoidal oscillations in figs. 1, 3, 4 and 5 as well as in global mean temperature [7] are superimposed on a gradually rising temperature trend. This rising trend seems to have started between 1600 and mid-1700's in unison with correspondingly rising sunspot number as may be deduced from figs. 6 and 7. Note the approximate coincidences of the maxima and minima in fig. 6 with those in fig. 7. While fig. 6 has maxima at years 1210 and 1580 as well as minima at 1460 and 1690, fig. 7 has maxima at 1220 and 1530 as well as minima at 1460 and 1640. Even the broad peak in fig. 6 extending from 3200 to 2300 B.C. coincides with a broad peak in "reconstructed" England and China temperatures [2].

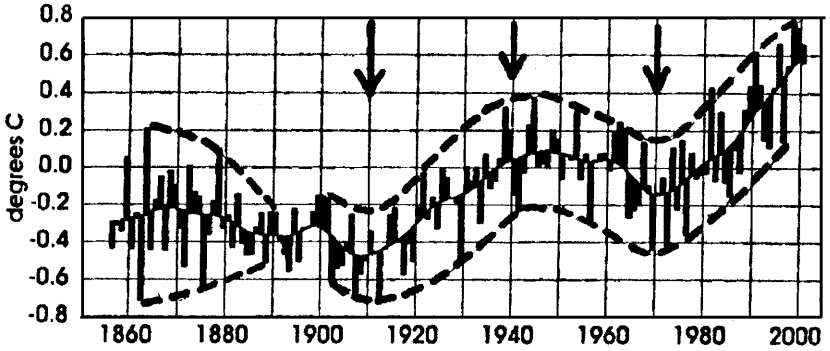

Fig. 5. – A plot of mean surface temperature in the part of the northern hemisphere north of latitude 30 °N from 1856 to 2000. The bars represent annual values as departures from the 1961–1990 mean. Also the smooth curve shows the result of filtering the annual values to reveal long-term fluctuations. Discontinuous lines have been used to sketch out the amplitude-modulation envelopes or states of the temperature variations using the curve-fitting techniques given in ref. [5]. The arrow-headed lines show timings of minima, maxima and the midpoint between a minimum and adjacent maximum in the solar cycle shown in fig. 2(b). Except for the discontinuous and arrow-headed lines, the plot has been derived from ref. [12].

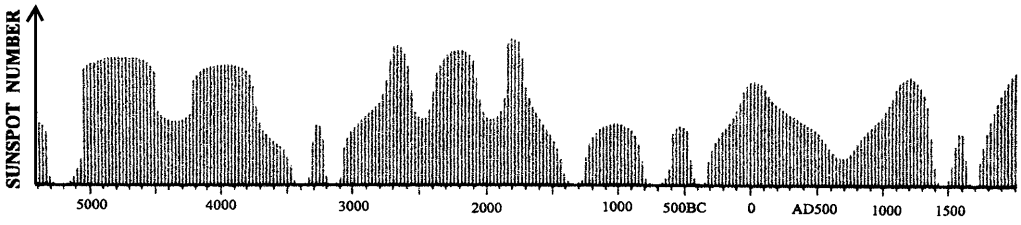

Fig. 6. – A plot of the long-term envelope of possible sunspot cycles since 5400 years B.C. as deduced from data on deviations in carbon-14 (from a diagram in ref. [14]).

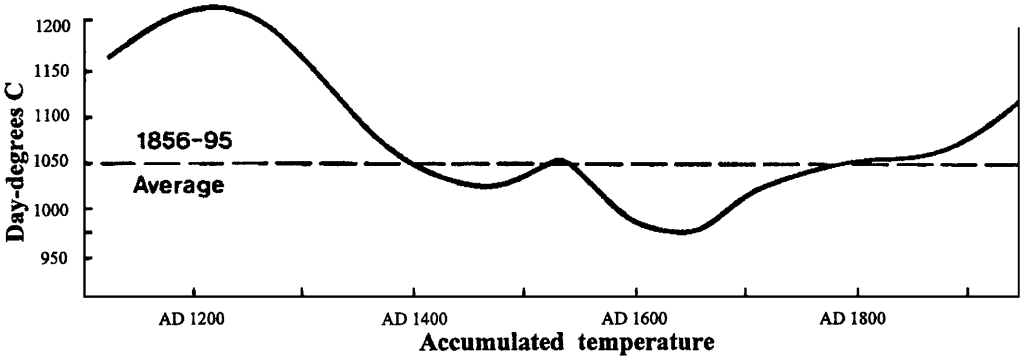

Fig. 7. – The estimated average accumulated warmth of the growing seasons prevailing at sites near the upper limit of cereal cultivation in the hill country of southeast Scotland in the period 1856–95 (discontinuous line) and its variations (solid line) over the last thousand years (from a diagram in ref. [2]).

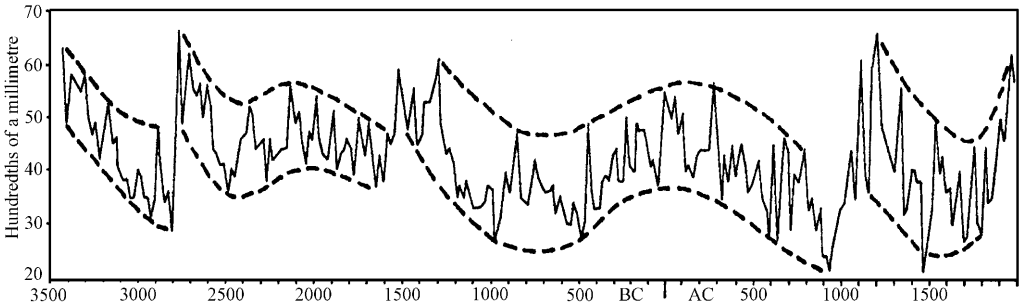

Fig. 8. – Ring widths (twenty-year averages) in the growth rings of Bristlecone pine trees near the upper tree line in the White Mountains, California since 3431 B.C. (solid lines) as adapted from Lamb [2]. The variations at this height may be taken as indicating variations of summer warmth and/or its seasonal duration. Discontinuous lines have been fitted through the maximum as well as minimum points using the curve-fitting techniques in ref. [5].

The time-length of the temperature record in fig. 7 is quite small compared with the time-length of the sunspot number record in fig. 6. We have, therefore, extracted from Lamb [2] some temperature record whose time-length is more than 75% of that of the sunspot number record in fig. 6. This particular temperature record is given in fig. 8. Except for the maximum at about 1800 B.C., all major maxima in fig. 6 coincide with major maxima in fig. 8. Also all major minima in fig. 6 approximately coincide with or just precede major minima in fig. 8.

As would be expected, the variations in fig. 7 are generally in unison with the corresponding variations in fig. 8. For example, the single major maximum (at year 1220 A.D.) and the single major minimum (at year 1640 A.D.) in fig. 7 coincide with a major maximum and a major minimum, respectively, in fig. 8.

Finally let us look at the major oscillations in fig. 8 and then find out whether any solar cycles are reflected in these oscillations. Major (sinusoidal) maxima exist in fig. 8 at the years 2050 B.C. and 100 A.D. Also major (sinusoidal) minima exist in fig. 8 at the years 2400 B.C., 700 B.C. and 1650 A.D. This series of maxima and minima indicate presence of a dominant oscillation with a mean period of 2070 years. As illustrated in fig. 8, this dominant oscillation is rapidly jerked upwards at about the years 2800 B.C., 1500 B.C. and 1000 A.D. The causes of these rapid upward-jerking episodes (*i.e.* rapid warming episodes) are given later on in the paper. It is interesting to note that the 2070-years oscillation which dominates in fig. 8 has a period that is approximately equal to that of the 2000-years solar cycle reported in Lamb [2].

As already mentioned earlier, another interesting feature in fig. 8 is that a major and rapid warming episode takes place during the second half of each falling phase of the $\sim$ 2070-years oscillation. Possible causes of the three rapid warming episodes shown in fig. 8 may be given as follows. Strictly speaking, the dominant oscillation sketched in discontinuous lines in fig. 8 has a period which changes with time, having a mean value of 2070 years. This oscillation generally varies in phase with the discontinuous line in fig. 9, the latter line representing long-period relative variations in the corresponding sunspot number patterns. We have noted earlier in connection with figs. 1 to 3 that the rapid changes indicated by arrowed lines in fig. 1 and fig. 3 take place due primarily to (and/or coincide with) significant changes in the frequency patterns of sunspot number. This implies that significant changes in the frequency pattern of sunspot number variations

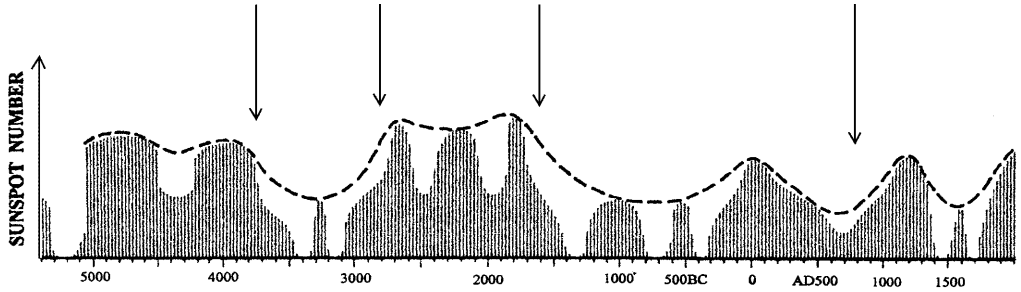

Fig. 9. – Same as fig. 6 but with the following additions: i) a discontinuous line has been fitted through the peaks of the sunspot number variations using the techniques given in ref. [5], and ii) arrow-headed lines have been inserted specifically to show timings of major frequency changes in the discontinuous line variations.

leads to rapid changes in (some) terrestrial temperature variations. In other words, a change in the frequency pattern of sunspot number acts as a switch for triggering rapid changes in (some) terrestrial temperature variations. It is noted along parallel reasoning that the three rapid warming episodes shown in fig. 8 coincide with (or are primarily due to) significant changes in the frequency pattern of the discontinuous line in fig. 9. Since this discontinuous line varies in unison with the dominant oscillation in fig. 8, we can predict when the next major maximum will occur in the California temperature variation patterns. From 700 A.D. onwards, the discontinuous line in fig. 9 shows a variation period of about 900 years. On this basis, the next major maximum is expected at about the year $1650 + 450 = 2100$. After arriving at the latter year, we low-pass filtered the variations in fig. 7 in order to remove all variations at periods less than 250 years. What remained after the filtering process was a large oscillation with a maximum at year 1220 and a minimum at the year 1660, with an implicit period of about 880 years. If we use this information in forward-extrapolating fig. 7, we reach at a conclusion that the post-1660 rising trend shown in fig. 7 will expectedly reach the next maximum at about the year $1660 + 440 = 2100$. Indeed, if global mean temperature patterns generally follow temperature patterns in Scotland and California, then we would expect major global cooling to start at about the year 2100.

We would like to end this section by noting generally that any significant change in the frequency (or frequencies) of sunspot number variations expectedly triggers rapid changes in terrestrial temperature patterns. These rapid changes may take the form of rapid increases (as in the case of central England temperature at about the years 1750 and 1925 in fig. 1), rapid drops (as in the case of central England temperature at about the year 1850 in fig. 1), rapid changes in amplitude-modulation modes (as in the case of global mean temperature at about the years 1875 and 1940 [8]), rapid phase changes or rapid changes in amplitudes. The theoretical and conceptual justification for this point of view (which is based on the contents in the Appendix) is as follows.

Whenever solar cycles dominate in terrestrial temperature patterns along the globe (or in a given region), these patterns are characterised by spatial arrangements or patterns of oscillations along the globe (or in region involved) with specific spatial wavelengths and solar cycle frequencies [7]. Now if there is a significant change in solar cycle frequencies, there must be a corresponding change in the spatial arrangements or patterns of the terrestrial oscillations in order to accommodate the new solar cycle frequencies. It is this

switch or adjustment from one spatial arrangement of terrestrial temperature oscillations into a different spatial arrangement which appears as a rapid change.

3. – General conclusion

We have shown that the dominant variations in England temperature and rainfall since 1726 are associated with solar activity. The envelopes of the variation patterns in both rainfall and temperature vary in unison with the sunspot number oscillation in fig. 2(b) before 1840. But after 1850 the changes in the latter envelopes are related to the changes in the discontinuous line in fig. 2(a). However, the 80–90 years switching pattern continues throughout the period covered by figs. 1 and 3. The largest radiative forcing due to changes in solar irradiance for the period since 1750 is estimated to be about $+0.3\,\mathrm{Wm}^{-2}$, most of which occurred during the first half of the 20th century. Also since the late 1970s, satellite instruments have observed small oscillations due to the 11-year solar cycle. Admittedly the solar effects just mentioned are too small to directly cause large temperature and rainfall changes such as those shown in figs. 1 and 3. But it has recently been found out (just before publication of the IPCC latest report [7, 15]) that some specific and theoretically justified mechanisms exist in the surface-atmosphere system (SAS) by which large heat/temperature oscillations which derive their energies from the (large) constant component of incoming solar energy are continuously formed in the SAS at the frequencies of the relatively small solar activity variations. To mere observers, this erroneously looks as if it is the small solar effects on climate which are greatly amplified [7]. Some rigorous observational basis for the mechanisms mentioned above is detailed in Njau [8]. Solar cycles are also reflected in California temperature records since 3431 B.C. Finally we have established that significant changes in the frequency (or frequencies) of sunspot number variations give rise to rapid changes in terrestrial temperature patterns.

* * *

We thank Prof. G. Williams, S. Nakagawa and B. E. Osborne for useful comments on an earlier version of this paper. We would also like to thank an anonymous referee for very useful suggestions which we have used to further improve the paper.

Appendix

Let R_0, R and $E(t)$ represent the mean Sun-Earth distance, the Sun-Earth distance at time t, and the earthward solar energy stream at time t, respectively. As the earth spins about its geographical axis, the arbitrary portion P of the surface-atmosphere system (SAS) located at latitude θ and longitude ϕ discretely samples off portions of $E(t)$ as it exposes itself ON (*i.e.* at daytime) and OFF (*i.e.* at night time) sequentially to energy stream $E(t)$. This ON-OFF energy sampling sequence is represented by $S(\theta, \phi, t)$. Let us assume that the above-mentioned SAS portion P at location (θ, ϕ) has net fractional absorption coefficients pattern associated with incident solar energy which is denoted by $A(\theta, \phi, t)$. Then the net solar and man-made energy $F(\theta, \phi, t)$ absorbed by portion P may be expressed as

$$F(\theta,\phi,t) = \left(\frac{R_0}{R}\right)^2 E_0(t) S(\theta,\phi,t) A(\theta,\phi,t) + \\ + H(\theta,\phi,t) + Q(\theta,\phi,t) + M(\theta,\phi,t), \tag{A.1}$$

where $E_0(t)$ is the form of $E(t)$ at distance R_0 from the earth, $H(\theta,\phi,t)$ is the Sun-derived energy transferred by convection and/or conduction into portion P from other SAS portions, $Q(\theta,\phi,t)$ is man-made energy generated at other SAS portions and transferred by any means into SAS portion P, and $M(\theta,\phi,t)$ is energy generated by man within portion P and then absorbed or left in this particular portion.

Let the t-dependent stretch of $F(\theta,\phi,t)$ from $t=0$ up to $t=T$ be denoted by $F_T(\theta,\phi,t)$. We may express $F_T(\theta,\phi,t)$ as follows:

$$\begin{aligned}(\text{A.2})\quad F_T(\theta,\phi,t) &= \left\{\left(\frac{R_0}{R}\right)^2 E_0(t)S(\theta,\phi,t)A(\theta,\phi,t) + H(\theta,\phi,t) + \right.\\ &\quad \left. + Q(\theta,\phi,t) + M(\theta,\phi,t)\right\}_{t \text{ from } 0\to T}\\ &= \big[E_0(t)JS(\theta,\phi,t)\big]_{t \text{ from } 0\to\infty} \times \left[\left(\frac{R_0}{R}\right)^2 A(\theta,\phi,t)\right]_{t \text{ from } 0\to\infty} +\\ &\quad + \big[H(\theta,\phi,t) + Q(\theta,\phi,t) + M(\theta,\phi,t)\big]_{t \text{ from } 0\to T},\end{aligned}$$

where

$$\begin{aligned} J &= 1, \quad \text{for } 0 \le t \le T,\\ &= 0, \ \text{otherwise}.\end{aligned}$$

If we take the influence of long-wave (terrestrial) radiation into consideration, then it can be shown (*e.g.*, see ref. [13]) that the overall and net energy pattern $F_G(\theta,\phi,t)$ that is absorbed at the SAS portion P from $t=0$ up to $t=T$ is given as

$$(\text{A.3}) \qquad F_G(\theta,\phi,t) = F_R(\theta,\phi,t)\left\{1 - \frac{b(\theta,\phi,t)[F_R(\theta,\phi,t)]^{\alpha-1}}{1+\alpha b(\theta,\phi,t)[F_R(\theta,\phi,t)]^{\alpha-1}}\right\},$$

where $F_R(\theta,\phi,t) = F_0(\theta,\phi,0) + F_T(\theta,\phi,t)$ such that $F_0(\theta,\phi,0)$ is the net and overall energy pattern existing at portion P at the "starting point" $t=0$, and $\alpha\,(\ge 1)$ is some numerical value. Since $E_0(t)$ consists of a huge constant component K_0 and tiny variable components, it may be expressed generally as

$$(\text{A.4}) \qquad E_0(t) = K_0 + \sum_{n=1}^{N} a_n \cos(\omega_n t + \Omega_n),$$

where a_n is a tiny amplitude, ω_n is the frequency of the n-th sunspot or solar cycle, Ω_n is a phase term and N is a positive integer.

If ω_d and V_d represent the frequency of the diurnal cycle and the variability of day-time duration, respectively, then

$$\begin{aligned}(\text{A.5})\quad &\big[E_0(t)JS(\theta,\phi,t)\big]_{t \text{ from } 0\to\infty} =\\ &= \left[K_0 + \sum_{n=1}^{N} a_n \cos(\omega_n t + \Omega_n)\right] \times\\ &\quad \times \big[h_1 \sin k_1\omega t + h_2 \sin k_2\omega t + h_3 \sin k_3\omega t + \cdots\big] \times\\ &\quad \times \big[C(\theta,\phi) + \big(\text{Variable series dependent on } \theta,\phi,t,\omega_d \text{ and } V_d\big)\big],\end{aligned}$$

where h_m and k_m are parameters that depend on the value of m, $C(\theta,\phi)$ is a non-zero constant at portion P, and $\omega = \pi/2T$. Thus frequencies $k_1\omega, k_2\omega, k_3\omega, \ldots$ gradually decrease as T and hence time increases. Remember that T was arbitrarily chosen as a specific value of t. By the way, parameter $C(\theta,\phi)$ is not a very small fraction. For example, $C(\theta,\phi) \approx 0.32$ in equatorial regions. Also the maximum value of h_m (for $m = l, 2, \ldots$) is 1.

Let the variations on the right-hand side of eq. (A.5) which are independent of ω_d be represented by $B(\theta,\phi,t)$. Then

$$\text{(A.6)}\quad B(\theta,\phi,t) = \left[K_0 + \sum_{n=1}^{N} a_n \cos(\omega_n t + \Omega_n)\right] C(\theta,\phi) \sum_{m=1}^{\infty} h_m \sin k_m\omega t$$
$$= \sum_{m,n} \Big\{ K_0 C h_m \sin k_m\omega t + \frac{1}{2} a_n h_m C \sin\big[(k_m\omega - \omega_n)t - \Omega_n\big] +$$
$$+ \frac{1}{2} a_n h_m C \sin\big[(k_m\omega + \omega_n)t + \Omega_n\big] \Big\}.$$

For any two given values, one for n and the other for m, frequency $(k_m\omega - \omega_n)$ is the smallest frequency in eq. (A.6) which decreases with time. Now as soon as the latter frequency decreases to zero, $k_m\omega = \omega_n$. Any further decrease in $k_m\omega$ without any "adjusting" processes would make frequency $k_m\omega - \omega_n$ negative, something which is not physically or practically possible. Physical attempts (like the one under consideration here) to create negative frequencies in actual oscillations by drifting the latter's frequency spectra from positive to negative frequencies inevitably trigger frequency-decreasing reversals (*e.g.*, through some phase reversals) in the oscillations which then make the follow-up frequencies positive instead of negative [16, 17]. The frequency-decreasing reversal occurs in $(1/2)a_n h_m C \sin[(k_m\omega - \omega_n)t - \Omega_n]$ as soon as $k_m\omega = \omega_n$ by changing the phase angle term $(k_m\omega - \omega_n)t$ to $-(k_m\omega - \omega_n)t$ before $k_m\omega$ continues to decrease further. This change i) reverses the frequency-decreasing process which has been occurring in $(1/2)a_n h_m C \sin[(k_m\omega - \omega_n)t - \Omega_n]$ before the condition $k_m\omega = \omega_n$ is attained; and ii) changes the pre-existing spectral relationships which had bound the three sinusoid terms on the right-hand side of eq. (A.6). Both processes i) and ii) above take place when $k_m\omega = \omega_n$, and it is after these time-consuming processes that further frequency changes follow. This frequency-decreasing reversal and hence phase-reversal phenomenon is well known in amplitude modulation processes as "cross-over distortion" in cases where variable frequency spectra attempt to cross the zero frequency line from positive to negative frequencies (*e.g.*, see refs. [16, 17]).

The frequency-decreasing reversal explained above may be put into simpler form as follows. Let the frequency spectrum of $(1/2)a_n h_m C \sin[(k_m\omega - \omega_n)t - \Omega_n]$ be represented by $Y(f,t)$, where frequency $f = k_m\omega - \omega_n$. As time passes, $Y(f,t)$ gradually drifts towards the zero-frequency line L_0 from the positive frequency side. On reaching line L_0, $Y(f,t)$ is reflected or turned back and made to reverse its motion and move in the opposite direction. But before $Y(f,t)$ reverses its direction of motion and start moving back away from line L_0 into the positive frequency side, it has to stop temporarily at line L_0. Indeed this is in line with basic motion/mechanics laws which dictate that a body moving along a straight line cannot reverse its motion on that line and move along the same straight line without temporarily stopping at the reversing point.

On the basis of the account just given above, we can conclude the following with regard to eq. (A.6) and two arbitrary values, one for m and the other for n.

i) As soon as $k_m\omega = \omega_n$, the decrease in $k_m\omega$ temporarily stops while a frequency-decreasing reversal takes place in $(1/2)a_n h_m C \sin[(k_m\omega - \omega_n)t - \Omega_n]$. It is also during this temporary stoppage that the spectral relationships binding the three sinusoids on the right-hand side of eq. (A.6) change.

ii) During the frequency-decreasing reversal and spectral relationships change processes mentioned in i) above, the large oscillation $K_0 C h_m \sin\omega_n t$ exists at the solar cycle frequency ω_n since $k_m\omega = \omega_n$.

iii) The large oscillation $K_0 C h_m \sin k_m\omega t$ exists for longer times at frequencies ω_n for $n = 1, 2, \ldots, N$ than at any other frequencies. Note that this is not a result of amplification of the tiny oscillations in $E_0(t)$. It is a result of "signal processing" changes which "leak" part of the energy contained in the large constant component of $E_0(t)$ into frequencies ω_n for $n = 1, 2, 3, \ldots, N$. This "leakage" occurs basically due to processes in the SAS which set up in order to ensure compliance with physical laws [16, 17] which disallow occurrence of negative frequencies.

It is well known that both $(R_0/R)^2$ and $A(\theta, \phi, t)$ have fairly large constant components. This realisation together with points i) to iii) above leads to the conclusion that $[E_0(t)JS(\theta, \phi, t)]_{t \text{ from } 0\to\infty} \times [(R_0/R)^2 A(\theta, \phi, t)]_{t \text{ from } 0\to\infty}$ in eq (A.2) and hence $F_T(\theta, \phi, t)$ and $F_G(\theta, \phi, t)$ continuously contain large oscillations at the frequencies of sunspot or solar cycles. If we assume a SAS albedo of about 0.34, the largest amplitude of these oscillations is about $0.21K_0$. These large solar cycles in $F_G(\theta, \phi, t)$ are mapped onto corresponding variations of the key meteorological parameters such as temperature and rainfall through well known physical processes (*e.g.*, see refs. [18, 19]).

REFERENCES

[1] Houghton J. T. *et al.* (Editors), *Climate Change 2001: The Scientific Basis* (Cambridge University Press, Cambridge) 2001.
[2] Lamb H. H., *Climate, History and the Modem World* (Methuen, London) 1982.
[3] Manley G., *Climate and the British Scene* (Collins, London) 1962.
[4] Lamb H. H., *The Changing Climate* (Methuen, London) 1966.
[5] The Curve Fitting Toolbox at www.mathworks.com/nncurvefitting visited on 01/10/2001.
[6] Paul M. and Novotna D., *Phys. Rev. Lett.*, **83** (1999) 3406. Also related collections obtained from the Internet http://science.nasa.gov/headlines/news_archive.htm on 10/08/2001.
[7] Njau E. C., *Proc. Indian Natn. Sci. Acad. A*, **66** (2000) 451.
[8] Njau E. C., *Proc. Indian Natn. Sci. Acad. A*, **66** (2000) 415.
[9] Marsh T. J., *Weather*, **56** (2001) 343.
[10] Hargreaves J. K., *The Upper Atmosphere and Solar-Terrestrial Relations* (Van Nostrand Reinhold Company, New York) 1979.
[11] Kukla G. J. and Robinson D. A., in *Climate Variations and Variability: Facts and Theories*, edited by Berger (D. Reidel Publishing Company) 1981.
[12] TIEMPO Issue 38/39 (June 2001) 38.
[13] Njau E. C., *Int. J. Renewable Energy*, **17** (1999) 319.
[14] Eddy J. A., *Climatic Change*, **1** (1977) 173.
[15] Njau E. C., *The fate of the snow on mount Kilimanjaro*, Tanzania Government Report (October 2001).
[16] Stark F., Tuteur F. B. and Anderson J. B., *Modern Electrical Communication* (Prentice-Hall, Englewood Cliffs, N.J.) 1988.

[17] Taub H. and Schilling D. L., *Principles of Communication Systems* (McGraw-Hill Book Company, New York) 1986.
[18] Peixoto J. P. and Oort A. H., *Physics of Climate* (American Institute of Physics, New York) 1992.
[19] Stevens W. K., *The Change in the Weather: People, Weather and the Science of Climate* (Delacorte) 2000.